

# Full-Scale Resistance Prediction in Finite Waters – A Study Using CFD Simulations, Model Test Experiments and Sea Trial Measurements

Max Haase, Gary Davidson, Jonathan Binns, Giles Thomas and Neil Bose

January 15, 2016

## Abstract

The development of large medium-speed catamarans aims increasing economic viability and reducing the possible negative influence on the environment of fast sea transportation. These vessels are likely to operate at hump speed where wave-making can be the dominating component of the total resistance. Shallow water may considerably amplify the wave-making and hence the overall drag force. Computational fluid dynamics (CFD) is used to predict the drag force of medium-speed catamarans at model and full scale in infinite and restricted water to study the impact on the resistance. Steady and unsteady shallow water effects that occur in model testing or full-scale operation are taken into account using CFD as they are inherently included in the mathematical formulations. Unsteady effects in the ship model response were recorded in model test experiments, CFD simulations and full-scale measurements and found to agree with each other. For a medium-speed catamaran in water that is restricted in width and depth, it was found that CFD is capable of accurately predicting the drag with a maximum deviation of no more than 6% when comparing to experimental results in model scale. The influences of restricted depth and width were studied using CFD where steady finite width effects in shallow water and finite depth effects at finite width were quantified. Full-scale drag from CFD predictions in shallow water ( $h/L = 0.12 - 0.17$ ) were found to be between full-scale measurements and extrapolated model test results. Finally, it is shown that current extrapolation procedures for shallow water model tests over-estimate residuary resistance by up to 12% and underestimate frictional forces by up to 35% when compared to validated CFD results. This study concludes that CFD is a versatile tool to predict the full-scale ship resistance to a more accurate extent than extrapolation model test data and can also be utilised to estimate model sizes that keep finite water effects to an agreed minimum.

## List of Symbols

---

### Roman

$A_x$	sectional area amidships	[m <sup>2</sup> ]
$b$	towing tank width	[m]
$C_F$	frictional resistance coefficient	[-]
$C_R$	residuary resistance coefficient	[-]
$C_V$	viscous resistance coefficient	[-]
$f$	motion frequency	[1/s]
$Fr$	length Froude number	[-]
$Fr_h$	depth Froude number	[-]
$g$	gravitational constant, 9.81	[m/s <sup>2</sup> ]
$h$	water depth	[m]
$(1 + k)$	form factor	[-]
$L$	ship length	[m]
$m$	blockage ratio	[-]
$R$	resistance force	[N]
$RF$	frictional resistance force	[N]
$RP$	pressure resistance force	[N]
$RR$	residuary resistance force	[N]
$RT$	total resistance force	[N]
$RV$	viscous resistance force	[N]
$S_W$	wetted surface area	[m <sup>2</sup> ]
$V$	ship velocity	[m/s]

---

### Greek

$\rho$	density	[kg / m <sup>3</sup> ]
$\lambda$	linear scale ratio	[-]
$\nabla$	volumetric displacement	[m <sup>3</sup> ]

# 1 Introduction

Large medium-speed catamarans are currently being developed to provide fast sea transportation with low environmental impact and high economic efficiency by increasing payload capacities and reducing service speed [1, 2, 3]. They are designed to efficiently operate around the main resistance hump where wave-making can be the main contributor to the overall resistance. However, at this particular speed range vessels are prone to encounter a significant increase in resistance when they operate in shallow water as the flow field around the vessel changes such that the effective flow velocity and wave-making increases [4, 5]. When considering the effect of shallow water, the influence of restricted water width may be considered as well. The physical effect of blockage that leads to an increased flow velocity around the hull is influenced by both limited depth and width. Consequently, the influence of finite waters on the vessel performance is addressed in this paper. Effects of finite water are not only measurable during ship operation, but also during performance prediction where the ship model can encounter steady and unsteady finite water effects which can potentially distort model test results. Steady finite water effects can lead to an increase in resistance due to increasing flow velocities as a result of blockage that is the limited canal cross section with respect to the vessels cross sectional area and due to increasing wave-making as a result of encountering low water depth that is expressed in terms of depth Froude number ( $Fr_h = V / \sqrt{g \times h}$ ). However, unsteady finite water effects lead to an increase in the period of oscillations in resistance and running attitude, namely sinkage and trim. They are known to occur in model testing and when mathematically describing the transient flow around the vessel [6, 7]. The oscillation period is dictated by the towing speed, but it can grow in shallow water so that less than one oscillation cycle may be recorded within one run which leads to inaccurate results when averaging the transient data record. According to model test experiments [8] the required effective power of a medium-speed catamaran can increase up to 55% at  $Fr = 0.45$  when the water depth drops to  $h/L = 0.24$ , and full scale measurements of [9] revealed that the necessary power can more than double if water depth drops to around  $h/L = 0.12 - 0.17$ . This implies a speed loss of a vessel with a propulsion plant designed to operate in deep water around hump speed of 13% and 25% for  $h/L = 0.24$  and 0.14. This emphasises that finite water can have a significant impact on the performance of medium-speed catamarans. Therefore, a reliable and universal prediction tool such as computational fluid dynamics (CFD) is desirable which is capable of accurately predicting drag in shallow water of conventional ships [10] and also of catamarans [11]. CFD inherently includes finite water effects as the governing flow physics are resolved and thus its impact on the vessel's performance at model and full scale.



Figure 1: Image of the 98 m INCAT high-speed catamaran.



Figure 2: Proposed design of a 130 m medium-speed catamaran.

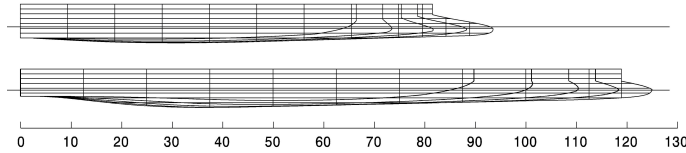


Figure 3: Line plans of the catamaran demihulls for the 98 m and 130 m vessel. Note that the lines are not drawn to scale.

## 1.1 Scope of Study

In an earlier study the use of CFD for full-scale drag prediction in conjunction with model-scale experiments was introduced [12]. This paper investigates the suitability of this method for use in finite water and also reports on steady and unsteady effects occurring in restricted waterways. Resistance prediction from physical model testing, numerical simulations, and also from full-scale sea trials of large medium-speed catamarans at varying water depth and width were utilised. Two case studies are presented featuring a 98 m and 130 m catamaran that can be seen in Figure 1 and 2 with lines plans shown in Figure 3. They aim is to show the difficulties that may arise in full-scale drag prediction for vessels in finite waters when using model test experiments and conventional ITTC procedures. RANS-based CFD is shown to be a suitable prediction tool for the total ship resistance in shallow water. It is concluded the CFD provides a more accurate prediction when compared to extrapolated model tests as the flow physics are resolved instead of relying on empirical

corrections and extrapolations.

## 2 Numerical Prediction Methodology

### 2.1 Numerical Simulation Tool

The current study utilised the RANS-based solver *interDyMFoam* of the OpenFOAM CFD toolbox (version 2.0, 2.3) for simulating the flow around a ship hull in shallow water. It includes 6 degree of freedom motion to enable dynamic trim and sink of the vessel travelling in viscous fluid with a free water surface. Close to the hull the flow was modelled by standard wall functions and the  $k - \omega - SST$  (shear stress transport) turbulence model. The influence of the cell count on the resistance was studied using the 130 m medium-speed catamaran. Computational meshes of different spatial resolution ranging from 660k to 1.3M cells when resembling towing tank dimensions were investigated. When compared to the results for the finest mesh, the drag force obtained from the coarsest mesh deviated by less than 1% for  $Fr = 0.37$  and less than 2.5% for  $Fr = 0.45$ , and the medium sized mesh differed by no more than 0.5% at both speeds. For this study a base mesh with a resolution adapted from the medium sized mesh was generated using the maximum considered width and depth. For smaller required values of width and depth the mesh was trimmed accordingly. Wave reflections at the outlet were avoided by using a flow rate driven boundary condition that adapts the outflow velocity to wave crest and trough situations.

### 2.2 Verification of numerical model

A 1:50 scale model of a 130 m catamaran was used to verify the results of the numerical prediction by comparing them to model test measurements in identical shallow water conditions of  $h/L = 0.24$ , where a depth Froude number of unity occurs at the resistance hump where the length Froude number equals 0.49. This can be considered as the worst case scenario for a vessel operating around hump speed.

The experiments were performed at the AMC towing tank (100 m  $\times$  3.8 m  $\times$  0.6 - 1.6 m) as reported by [8]. Here, results at Froude numbers of  $Fr = 0.37$  and 0.45, which correspond to depth Froude numbers of  $Fr_h = 0.76$  and 0.92, are considered. The results were determined for a light and heavy displacement corresponding to  $L/\nabla_{dh}^{1/3} = 10.2$  and 11.7 and results of numerical and experimental predictions can be seen in Figure 5. The uncertainty of the experimental drag prediction varies between 1 and 3 % [13]. They were non-dimensionalised by displacement, density and gravity ( $R' = R / (\nabla \times \rho \times g)$ ). The total drag obtained from model test experiments was subdivided into a frictional part (RF, as determined by ITTC model-ship correlation line) and residuary resistance (RR). Numerical results were divided into drag from shear stresses (RV) and normal pressure (RP). Numerical values for the relative difference between CFD and model test predictions with respect to experimental results ( $R_{T(CFD)}/R_{T(EXP)} - 1$ ) are presented in Table 1 and a

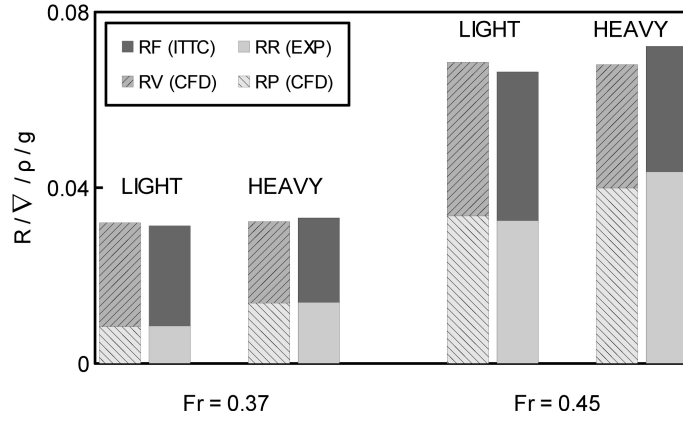


Figure 4: Calm water resistance of a 1:50 scale model of the 130m medium-speed catamaran in shallow water ( $h/L = 0.24$ ) for  $Fr = 0.37, 0.45$  for heavy and light displacement subdivided into a frictional (RF, RV) and pressure related components (RR, RP).

Table 1: : Relative difference between numerical simulations and towing tank results of the 1:50 130 m catamaran. Negative values indicate that the CFD result is below the experimentally determined value.

Relative deviation of resistance components: CFD vs model scale experiments						
$Fr$	LIGHT			HEAVY		
	$RT/RT - 1$	$RV/RF - 1$	$RP/RR - 1$	$RT/RT - 1$	$RV/RF - 1$	$RP/RR - 1$
0.37	0.022	0.037	-0.019	0.033	0.033	0.033
0.45	-0.025	-0.036	-0.010	-0.058	-0.016	-0.085

deviation below 6% was achieved. This is as an acceptable accuracy, because the largest deviations occur at  $Fr = 0.45$  where the depth Froude number approaches unity ( $Fr_h = 0.92$ ), where uncertainties in model testing increases and the drag force does not converge as it does at lower speeds or deeper water. These unsteady effects are discussed below in section 3.2.

### 3 Finite Water Effects

Water restricted either in depth or width can influence the vessel performance due to an increased flow velocity around the vessel which is considered as blockage. Also increased wave-making will occur if the combination of speed and water depth results in a critical depth Froude number close to unity, which is defined as  $Fr_h = V / \sqrt{g \times h}$  with  $h$  being the water depth. While this is a steady effect, an unsteady phenomenon occurs, due to the full-scale ship or towing tank model acceleration, which causes oscillatory behaviour for the drag, sinkage and trim.

#### 3.1 Steady Finite Water Effects

A numerical investigation into the effect of restricted water on the steady state drag force in model scale testing is reported in this section. Model scale results from CFD or physical testing may be influenced by the limited width and depth of the experimental facility, which do not concur with the prospective operational conditions of the full scale-vessel. Especially for vessel operation around hump speed the power requirements may double in shallow water conditions compared to deep water and therefore insights into performance variations due to finite waters are of great importance [9]. Furthermore, it was found that shallow water effects are more pronounced for vessels at a heavier displacement [9, 8].

##### 3.1.1 Finite Width Effects

Firstly, the influence of the domain width on the resistance of a 130 m medium-speed catamaran [8] was numerically studied for  $b/L = 1.4, 3.5$  and  $8.75$  for a shallow water case at  $Fr = 0.37$  and  $0.45$  with  $h/L = 0.24$ . This corresponds to depth Froude numbers of  $Fr_h = 0.76$  and  $0.92$ . The resistance was determined at three different domain widths and a value for an infinitely wide tank was determined using the generalised Richardson extrapolation. At  $Fr = 0.37$  and  $b/L = 1.4$  the residuary resistance was 15% above the value for an infinitely wide tank and below 1% for  $b/L = 3.5$  and  $8.75$ . For the higher speed at  $Fr = 0.45$  the residuary resistance was above the value for an infinitely wide domain by 39%, 10% and 2% for  $b/L = 1.4, 3.5$  and  $8.75$ . At  $Fr = 0.45$  the depth Froude number is close to unity, which may cause a significantly lower order of convergence when compared with cases for lower Froude depth numbers. The results are summarised in Table 2 where the relative difference in residuary resistance compared to an infinitely wide domain (finite vs infinite depth) is expressed as:  $C_R(b/L) / C_R(b/L = \infty) - 1$ . Figure 5 shows the convergence of residuary resistance with increasing domain width for  $h/L = 0.24$  indicated by grey lines.



### 3.1.2 Finite Depth Effects

Secondly, the influence of varying water depth on the resistance was studied at a constant tank width of  $b/L = 1.4$ . The model of the 130 m medium-speed catamaran [8] was simulated at  $h/L = 0.24, 0.6$  and  $1.5$  at  $Fr = 0.37$  and  $0.45$  with the effective depth Froude number varying from  $Fr_h = 0.30$  to  $0.93$ . A value for infinitely deep water was determined using the generalised Richardson extrapolation.

At  $Fr = 0.37$  the residuary resistance was 15% and 2% above that of an infinitely deep tank for  $h/L = 0.24$  and  $0.60$  and 167% and 3% at  $Fr = 0.45$ . For  $h/L = 1.5$  no significant difference was observed in either of the two speeds under investigation. The results are plotted in Figure 5 as black lines.

For the original tank depth ( $h/L = 0.6$ ) the residuary resistance decreased by 2% and 3% for  $Fr = 0.37$  and  $0.45$  when extending  $b/L$  from  $1.4$  to  $2.5$ . These values were identical to those obtained for the infinitely deep tank. The results are summarised in Table 2 where the relative difference in residuary resistance compared to an infinitely deep domain (finite vs. infinite depth) is expressed as:  $C_R(h/L) / C_R(h/L = \infty) - 1$ . The results lead to the conclusion that the water depth needs to be at least  $0.7 \times L$  and  $0.8 \times L$  for  $Fr = 0.37$  and  $0.45$  to reduce a deviation of residuary resistance by no more than 1% when compared to an infinitely deep domain at the width of  $b/L = 1.4$ . In shallow water conditions at  $h/L = 0.24$  the width of the fluid domain needs to be at least  $1.2 \times L$  for  $Fr = 0.37$  to not exceed an increase in resistance of more than 1%, when compared to an infinitely wide domain. However, as shown by the low convergence for  $Fr = 0.45$  for  $h/L = 0.24$  the domain width is required to be at least  $15.6 \times L$  for an increase in residuary resistance not to exceed 1%.

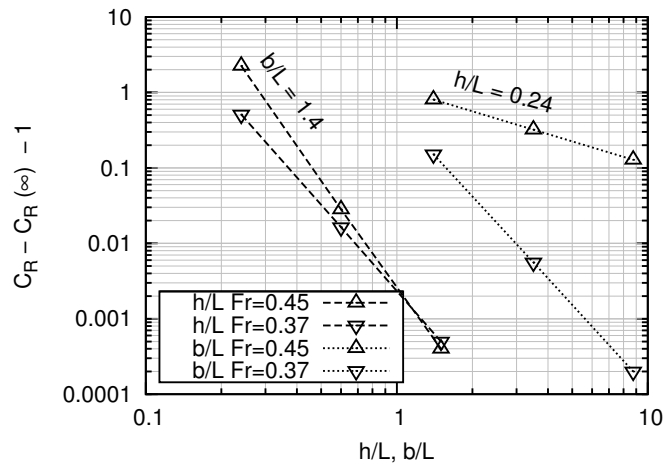


Figure 5: Convergence of residuary resistance of a 130 m catamaran at 1:50 model scale with respect to varying tank dimensions for  $Fr = 0.37$  and  $0.45$ . The black lines show the relative difference of residuary drag at varying tank depth at original tank width ( $b/L = 1.4$ ) compared to an infinitely deep tank. The grey lines represent the relative difference of residuary drag for different values of tank width in shallow water conditions ( $h/L = 0.24$ ) compared to an infinitely wide tank.

Table 2: Comparison of drag force at different length and depth Froude numbers of the 130 m catamaran At 1:50 model scale. \* Indicates relative difference to  $b/L = 3.8$  instead of  $b/L = \infty$ .

$Fr$	$h/L$	$Fr_h$	$b/L :$	Relative deviation of $C_R$ :			
				finite vs. infinite width		finite vs. infinite depth	
				1.4	3.8	8.75	1.4
0.37	1.50	0.30		-	-	-	0.00
	0.60	0.48		0.02*	-	-	0.02
	0.24	0.76		0.15	0.01	0.00	0.51
0.45	1.50	0.37		-	-	-	0.00
	0.60	0.58		0.03*	-	-	0.03
	0.24	0.92		0.60	0.17	0.05	1.67

### 3.2 Unsteady Finite Water Effects

The time series of calm water model test data shows a distinct frequency response in unsteady trim and resistance as shown in Figure 6 and 7. [14] derived a closed form solution for the oscillation period of the resistance force of a steadily moving two-dimensional source and [6] for a three-dimensional surface vessel when accelerated from rest. Both concluded that the period of oscillation ( $1/f$ ) of the resistance force can be calculated using:

$$1/f = 8 \times \pi \times V / g$$

This effect can be explained by waves that are diverging away from the moving vessel which were created by a disturbance, such as due to a change in speed (i.e. model acceleration), wave encounter or trim tab deflection. In deep water, the phase velocity of this wave is always twice the vessel velocity, which results in a following wave situation where the resulting wave encounter period can be estimated by the above formulation. It was shown that the amplitude of this wave decays at a certain rate [6]. More recently, [7] investigated the effect of shallow water on the oscillation period and derived a correction for the motion period from model test experiments using a Wigley hull that depends on the depth Froude number ( $Fr_h$ ) which is applicable for  $Fr_h > 0.2$ :

$$f / f_0 = \sum_0^6 (a_i \times Fr_h^i)$$

with  $a_i = (1.273; -4.365; 26.12; -72.29; 95.45; -63.82; 17.64)$ . The motion period increases in shallow water with increasing  $Fr_h$  and reaches infinity at  $Fr_h = 1$ , because the model speed and the phase velocity of the wave created by the disturbance are identical. [7] advised that this pitch motion may influence the resistance

prediction in a towing tank of finite length, because an integer number of motion cycles need to be resolved to determine a reliable average of the measured resistance force. Furthermore they point out that the decay rate of the oscillations in shallow water is significantly smaller than that in deep water.

The 98 m wave-piercing high-speed catamaran with slender demihulls of 1:22 model scale at water depth of  $h/L = 0.35$  was tested in the *AMC* towing tank at pre-hump speeds as presented in [12]. Figures 6 and 7 show values of trim and resistance for  $Fr = 0.31, 0.39$  and  $0.44$ . The data was filtered using a 1 Hz low-pass filter and normalised by the average value. For the pitch motion it can be observed that an increase in velocity leads to an increased motion period ( $1/f = 6.8, 12.5, 21.4$  s for  $Fr = 0.31, 0.39, 0.44$ ) and reduced motion amplitude. While the pitch amplitude varies up to  $\pm 15\%$  compared to its average value, for  $Fr = 0.44$  it varies up to  $\pm 40\%$  for  $Fr = 0.31$ . The resistance fluctuates in phase with the trim, up to  $\pm 5\%$  for all three speeds under consideration.

[15] reported that distinct pitch motions occur for both the model-scale and full-scale vessel. While the first were recorded using an LVDT (linear variable differential transducer) in towing tank measurements, the latter were obtained from strain gauge measurements of the superstructure of the vessel during sea trials. The investigations of [15] were based on a 112 m INCAT wave-piercing catamaran that can be considered as being similar to the 98 m and 130 m vessel presented in this study. Figure 8 shows the motion frequency normalised by  $\sqrt{g/L}$  of the 112 m catamaran at 1:17 and 1:45 model and full scale as well the frequency of a 130 m catamaran at 1:50 model scale and a 98 m catamaran at 1:22 model scale. The water depth varied from  $h/L = 0.24 - 1.75$ . The motion frequency from CFD results agrees to those obtained by model test experiments. It can be clearly observed that the non-dimensional frequency reduces with increasing length Froude number and decreasing water depth. Also the estimates obtained from [14], including shallow water corrections from [7], were plotted in Figure 8 and excellent agreement over a wide range of cases can be seen.

Furthermore, it was found that the pitch frequency at zero speed, which is solely dictated by hydrostatic properties of the hull is in alignment with the data recorded for the steadily travelling vessel. However, the oscillation of ship attitude and resistance during the transient resistance prediction process is different from hydrostatically restored ship motion such as the oscillations at zero speed. The oscillations for a steadily moving vessel result from an excitement of the vessel by waves that were created by a disturbance from the vessel due to its acceleration. Additionally, numerical simulations were used to determine the pitch frequency at infinitely deep water conditions. The hull of a 130 m medium-speed catamaran was simulated at  $Fr = 0.37$  at three different depths and constant width and the resulting motion frequency measured. It resulted in  $T = 14.2, 6.0$  and  $4.8$  s for  $h/L = 0.24, 0.6$  and  $1.5$ . When using generalised Richardson extrapolation a period for infinite depth was estimated to be  $1/f = 4.6$  s which agrees to the values predicted

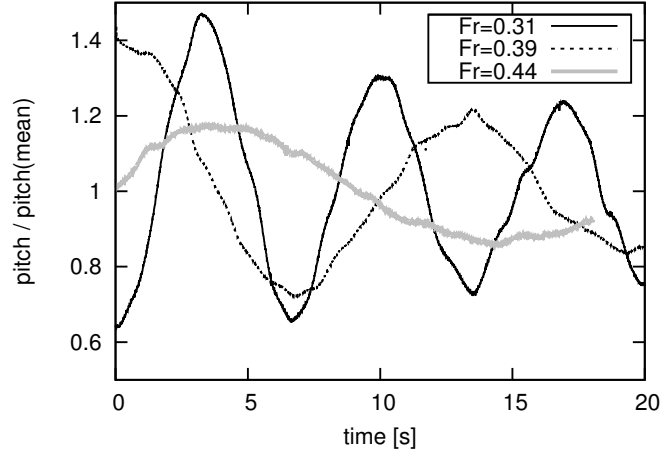


Figure 6: Fluctuation of trim for 1:22 model of slender catamaran normalised by its average value for  $Fr = 0.31, 0.39$  and  $0.44$  during towing tank run.

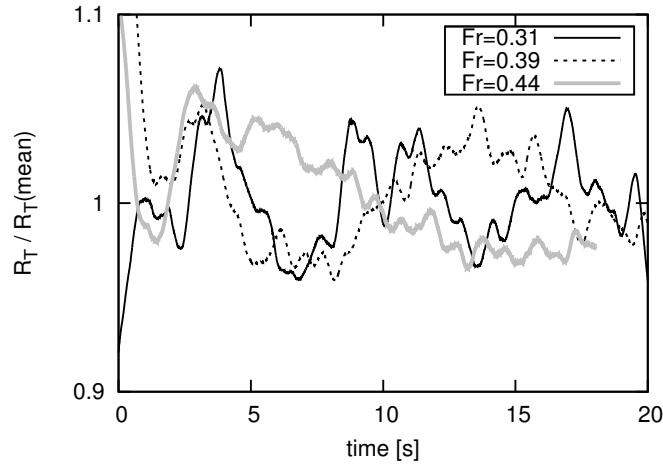


Figure 7: Fluctuation of drag force for 1:22 model of slender catamaran normalised by its average value for  $Fr = 0.31, 0.39$  and  $0.44$  during towing tank run.

by [14].

It was found that the period for oscillations in model test measurements and CFD simulation results was comparable at identical speeds. This occurs even though in towing tank experiments the model is steadily accelerated from rest, while in the CFD simulations the model is suddenly exposed to a flow at a constant speed. [16] showed that applying springs and dampers to the catamaran model in CFD simulations does not affect these oscillations, only reducing the acceleration of the model leads to a decrease in magnitude of the fluctuations of vessel response.

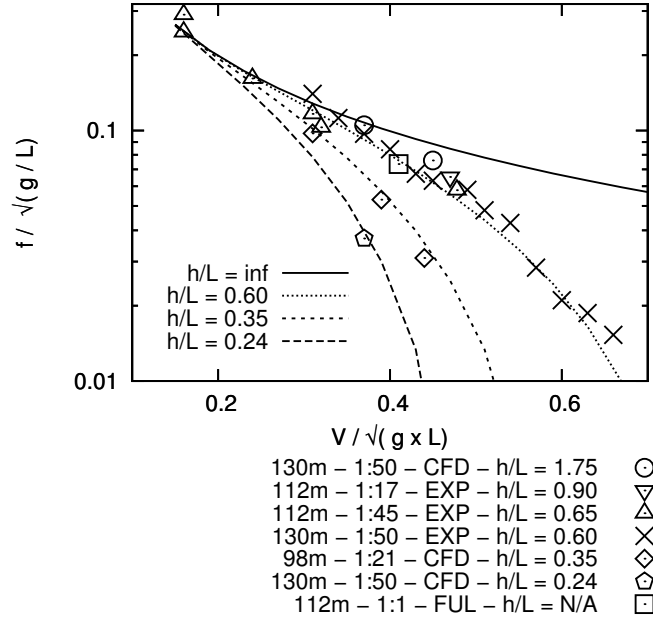


Figure 8: Non-dimensional calm water pitch frequency with respect to length Froude number from model test experiments (EXP), numerical simulations (CFD) and full-scale measurements (FUL) for different water depths. The lines present the prediction by [14] (solid line) and corrections for shallow water effects as proposed by [7] for  $h/L = 0.24$  (long dashed line)  $h/L = 0.35$  (normal dashed line) and  $h/L = 0.6$  (short dashed line).

## 4 Implications on Full-Scale Resistance

### 4.1 Full-Scale CFD Approach

The methodology to predict the full-scale drag at model-scale dimension proposed in [12] has been extended to take shallow water effects into account. To determine the full-scale resistance of a vessel the fluid domain needs to be modelled in accordance to:

- obtain a near wall modelling that is independent of Reynolds number;
- replicate cross sectional dimensions of towing tank.

The first can be achieved if the first cell height is chosen to be  $y_1 = 0.6 \times L \times 10^{-6}$ , as shown previously in [12], while the latter needs to be fulfilled to account for steady finite water effects such as blockage and increased wave making.

The results from CFD simulations at model scale are compared with model test experiments with corresponding linear dimensions and fluid properties. If the total resistance agrees and the wall shear stress coefficient is close to that of the ITTC model-ship correlation line ( $CV = CF$ ) or established friction lines, the numerical results can be considered as being valid. Therefore, it is assumed that both, pressure and viscosity related drag are correctly predicted. Also, it is assumed that the accuracy of the pressure resistance is independent of Reynolds number, hence the same mesh close to the ship hull can be used for full-scale simulations. Full-scale Reynolds numbers are achieved by altering the viscosity of the fluid rather than by scaling linear dimensions. Before conducting the full-scale simulation, steady finite water effects may need to be taken into account and any of the following cases can be considered:

- Model-scale testing and full-scale operation are in finite waters, with relative depth and width being identical at both scales.
- Finite water is present for verification at model scale, but the water can be considered as being infinite for the full-scale ship
- Unrestricted water applies for the verification at model scale, but the full-scale ship operates in finite water.
- Model and full-scale vessel sail in finite waters, but depth and width are not in correlation between scales.

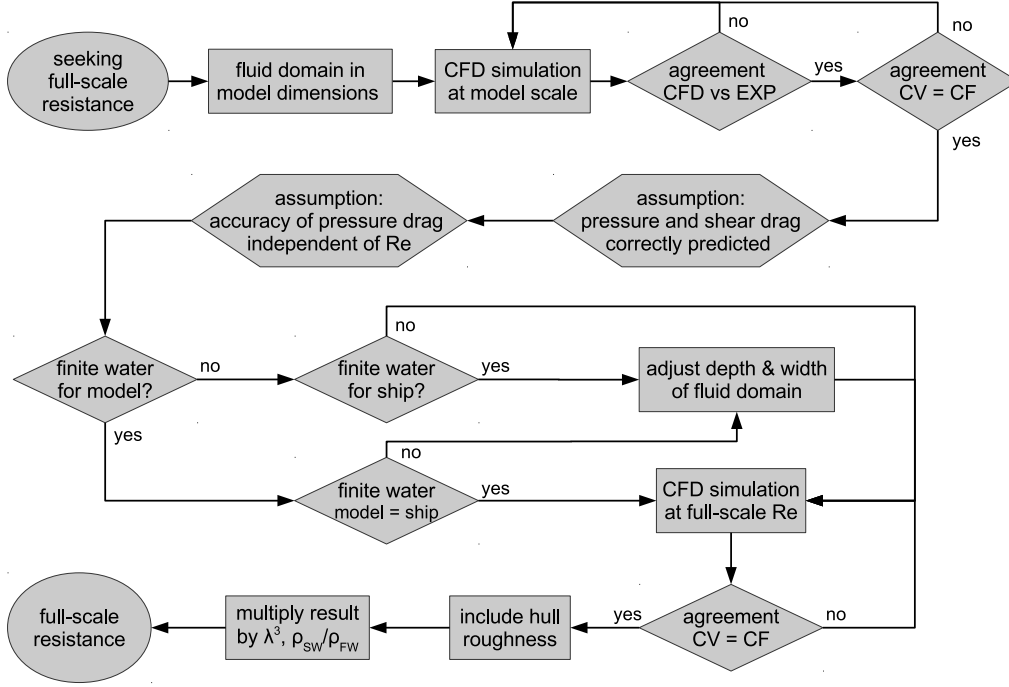


Figure 9: Flowchart to obtain full-scale resistance considering shallow water effects using a novel CFD approach in conjunction with model test experiments for verification.

If the first case applies, the identical mesh can be used for model and full-scale simulations, however, if any of the latter three cases apply the absolute dimensions of the computational domain need to be adjusted accordingly to assure that the influence of finite water on the full-scale results is physically correct.

The full-scale simulation can be run for a smooth hull and considered as being accurate when an acceptable agreement of the shear force coefficient with a model-ship correlation line or friction line is achieved ( $CV = CF$ ). If desired, the surface roughness can be taken into account in terms of equivalent sand grain roughness. To finally obtain dimensional full-scale resistance the result needs to be multiplied by scale factor to the power of three and the relative difference of fluid density between model and full scale ( $\rho_{SW} / \rho_{FW}$ ). The approach is summarised in Figure 9.

## 4.2 Case Study of a 98 m Catamaran

In this section the numerically determined full-scale drag of the 98 m catamaran is compared to results from power measurements from sea trials [9] and extrapolated model test data. The full-scale resistance from the shaft power measurements was derived using thrust curves of the waterjet propulsors, neglecting the effects of wake fraction and thrust deduction as shown in an earlier study [12]. The model test data was extrapolated using ITTC guidelines including shallow water corrections, of [4]. The validation was performed at a speed of 18 knots which corresponds to a length Froude number of  $Fr = 0.31$  and for  $h/L = 0.12 - 0.17$  to a depth

Froude number of  $Fr_h = 0.79 - 0.92$ .

#### 4.2.1 Extrapolation of Model Test Data

The model test data of the 98 m catamaran presented in [12] was extrapolated using ITTC procedures (7.5-02-02-01) with  $(1 + k) = 1.0$  and the correction of [4] applied to account for shallow water effects. The approach was utilised first to obtain data applicable in infinite water from resistance tests that were conducted in finite water ( $h/L = 0.35, b/L = 1.4$ ). Secondly the resistance for the vessel in infinitely wide, but shallow water ( $h/L = 0.12 - 0.17, b/L = \infty$ ) was estimated using the approach by [4] where the ship speed with respect to the resting water is corrected, which is defined as follows:

$$dv/V = m / (1 - m - Fr_h^2) + (1 - R_F/R_T) \times 2/3 \times Fr_h^{10} \quad (1)$$

with  $m = A_x/(b \times h)$  where  $m$  is the blockage ratio with  $A_x$  being the cross sectional area of the hull. The term  $(1 - R_F/R_T)$  predicts the portion of wave-making to which the correction addresses.

Furthermore, an empirically determined roughness and correlation allowance as proposed by ITTC (7.5-02-02-01) was added with  $200 \mu\text{m}$  of equivalent sand grain roughness. Wind drag, based on measurements by [17], was utilised to make the data comparable to estimates from sea trial measurements.

#### 4.2.2 Comparison of Results

The full-scale resistance of a 98 m high-speed catamaran in shallow water was investigated at  $Fr = 0.31$ . The sea trials were run at a depth ranging between  $0.12 < h/L < 0.17$ . The predictions were made at the two extreme values of depth. While a finite depth was modelled in CFD, the correction of [4] was applied to the model test data before corrections for shallow water and blockage (to be applicable for deep water) using the same approach.

Relative differences between predictions from CFD and model tests compared to sea trial data were made by  $R_{T(CFD)}/R_{T(seatrial)} - 1$ , with results presented in Figure 10 Table 3. The drag forces from the CFD predictions were 17% and 32% below the values estimated from the full-scale sea trials, with the extrapolated data being 33% and 40% below the results from sea trials. If no shallow water correction during the extrapolation was applied the deviation reached up to 42%. These differences are significantly larger than those obtained in deep water conditions presented in earlier work [12].

Possible reasons for these discrepancies between the results from CFD and sea trials may be an increased uncertainty in sea trials due to unsteady effects in finite water, or the effect of wake fraction and thrust



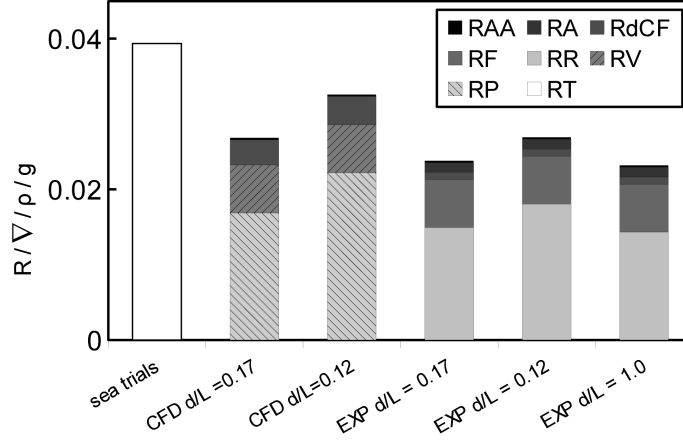


Figure 10: Dimensionless drag at  $Fr = 0.31$  obtained from CFD and model test extrapolation for two depths which were stated as extreme values for the sea trial measurements. Drag in deep water was added for comparison.

Table 3: Relative deviation of predicted full-scale drag for 98 m catamaran using CFD and extrapolated model test data corrected for shallow water by approach of [4] without form factor with respect to drag estimated from full-scale powering measurements.

		Relative deviation of $R_T$ : CFD and model test extrapolations vs. sea trials				
speed		CFD		model test		
[kn]	$h/L$ :	0.17	0.12	0.17	0.12	1.0
18.2		-0.32	-0.17	-0.4	-0.33	-0.42

deduction being insignificant which cannot be assumed as being valid under the current conditions. Based on the successful verification of shallow water drag force, the authors assume a comparable accuracy for the full-scale drag when predicted by CFD. Since for  $Fr = 0.31$  the deviation in drag increased from 10% in deep water [12] to 17% and 32% in shallow water, the origin may be concluded to result from changing flow into the waterjet units and hence an increased thrust deduction or reduced propulsive efficiency.

Furthermore, the presented results lead to the conclusion that the model test extrapolation, including shallow water corrections, significantly underestimates the full-scale drag, which implies that the approach by Schuster is not necessarily valid to accurately predict shallow water drag of a vessel from data that was recorded in deep water towing tank experiments.

### 4.3 Case Study of the 130 m Catamaran

The full-scale resistance for the 130 m catamaran when considered a smooth hull was predicted in shallow water and compared to extrapolated model test data that was recorded in shallow ( $h/L = 0.24$ ) and deep water condition ( $h/L = 0.6$ ) and extrapolated according to ITTC guidelines (7.5-02-02-01). The deep water data was extrapolated with and without considering shallow water corrections proposed by [4].

$$R_R = C_R \times \rho/2 \times (V \times (1 + dv/V))^2 \times S_W \quad (2)$$

where  $dv/V = 2/3 \times Fr_h^{10}$  as  $m = 0$  for an infinitely wide fluid domain. However the numerical simulation revealed that the flow velocity around the vessel can increase up to 6% for  $Fr_h = 0.92$  at  $h/L = 0.24$  in a sufficiently wide tank of  $b/L = 8.75$  where no interaction with the side wall was observed. The model-scale experiments were conducted at a tank width of  $b/L = 1.4$ , however, due to the findings in Section 3.1 the full-scale simulation was conducted at  $b/L = 3.8$  and  $8.75$  for Froude numbers of  $Fr = 0.37$  and  $0.45$ .

#### 4.3.1 Comparison of Drag for the 130 m Catamaran

Figure 11 shows the results for a smooth hull based on numerical simulations and extrapolated model test data from deep and shallow water runs. The experimental data for both speeds was obtained at a tank width of  $b/L = 1.4$ , while in the numerical simulations the tank width was  $b/L = 3.5$  for  $Fr = 0.37$  and  $b/L = 8.75$  for  $Fr = 0.45$  based on the results from the study in section 3.1.2 on finite width effects to minimise their impact. The deviation between the resistance prediction by CFD and shallow water experiments is 11% and -3.5% at  $Fr = 0.37$  and  $0.45$  as summarised in Table 4. When considering the resistance components from the data obtained at  $h/L = 0.24$  (see Table 5), it can be seen that the pressure related drag (RP, RR) is 5%

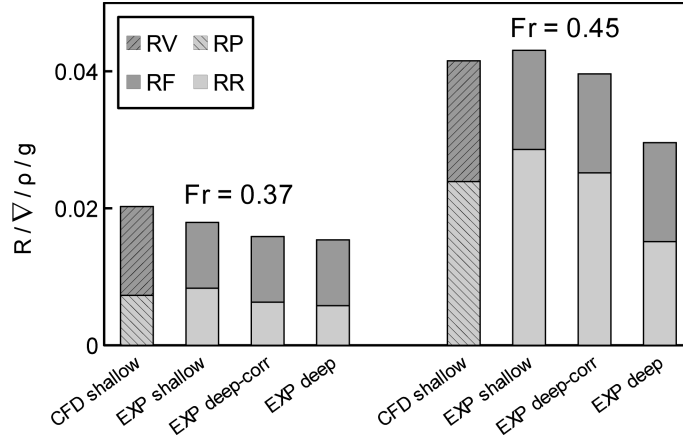


Figure 11: Full scale drag predictions for 130 m catamaran from model test experiments and CFD of bare hull with no superstructure of 130m medium-speed catamaran at  $Fr = 0.37$  and  $0.45$  in shallow water. Model test results were obtained at shallow water (EXP-shallow) and deep water with (EXP-deep-(S)) and without (EXP-deep) correction for shallow water by approach of Schuster (S).

Table 4: Relative differences of extrapolated model scale results compared to CFD predictions for full-scale resistance of 130 m medium-speed catamaran in shallow water at  $h/L = 0.24$ . Positive values indicate higher prediction by CFD, model test data has been recorded in shallow  $h/L = 0.24$  and deep water  $h/L = 0.60$  including the latter corrected by the approach of Schuster [4].

			Relative deviation of $R_T$ : CFD vs. model test extrapol.		
depth correction:			none	Schuster	none
$Fr$	$Fr_h$	$h/L$ :	0.24	0.6	
0.37	0.58		0.11	0.22	0.24
0.45	0.92		-0.04	-0.05	0.29

and 12% lower in CFD results while the frictional part (RF, RV) is higher by 35% and 21% in numerical predictions for the lower and higher speeds respectively. In deep water the deviation in pressure related drag was similar, but the frictional was different only by 1% and -5% when compared to the results of simulations and extrapolated experiments without using a form factor (compare to [12]).

The extrapolated resistance data from deep water runs under estimates the numerically predicted drag by up 38% for  $Fr = 0.45$  when no shallow water correction is applied.

The CFD-predicted resistance showed larger deviations when compared to extrapolated model test data than it was achieved in deep water conditions as presented earlier research [12]. Numerically-predicted residuary or pressure drag is lower than that experimentally determined, while the opposite is true for the viscous or frictional resistance part. Since the deviation in drag between model-scale results and CFD simulations is below 3% it can be assumed that CFD is capable of accurately resolving the flow around a vessel in shallow water. The differences in total drag and especially of the frictional component when

Table 5: Relative Differences Of Extrapolated Model Scale Results Compared To CFD Predictions For Full-scale Resistance Of 130 m Medium-speed Catamaran In Shallow Water At  $h/L = 0.24$ . Positive Values Indicate Higher Prediction By CFD, Model Test Data Has Been Recorded In Shallow  $h/L = 0.24$  And Deep Water  $h/L = 0.60$  Including The Latter Corrected By Approach Of [4].

$Fr$	Relative deviation of resistance components CFD vs. model test extrapol.		
	RT/RT-1	RP/RR-1	RV/RF-1
	RT/RT-1	RP/RR-1	RV/RF-1
0.37	0.11	-0.05	0.35
0.45	-0.04	-0.12	0.21

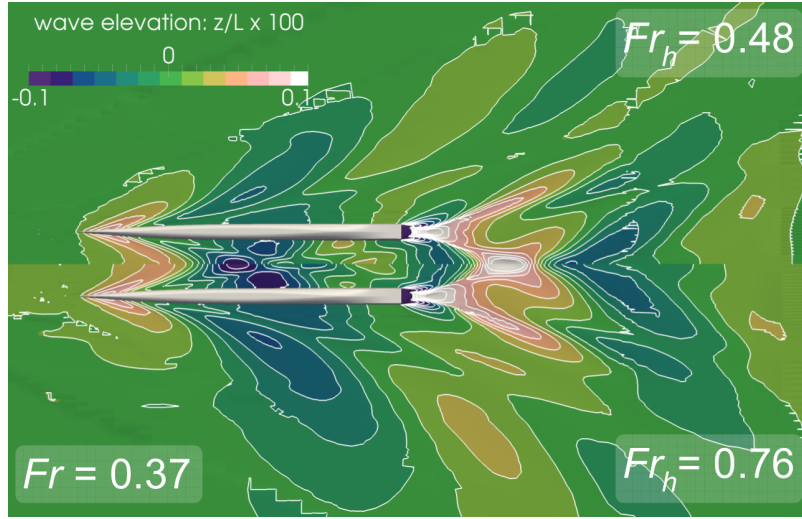


Figure 12: Wave contour of the 130 m catamaran at 1:50 model scale at  $Fr = 0.37$ . Top:  $h/L = 0.6$ ,  $Fr_h = 0.48$ . Bottom:  $h/L = 0.24$ ,  $Fr_h = 0.76$ .

comparing the results of CFD and extrapolated model tests applicable to the full scale ship may lead to the conclusion that ITTC recommended procedures for model test extrapolation are not readily applicable for shallow water conditions.

#### 4.3.2 Comparison of Wave-making for the 130 m Catamaran

Figure 12 and 13 show the difference in the free surface elevation for a reduction in water depth from  $h/L = 0.6$  to  $h/L = 0.24$  at Froude numbers of 0.37 and 0.45. In Figure 12, an amplification in wave height can be observed, whereas a more severe impact can be seen in Figure 13. When the depth Froude number approaches unity, a large wave trough builds up in the stern region of the catamaran. This clearly demonstrates that for such high depth Froude numbers, empirical corrections for the flow velocity may not be sufficient to accurately take shallow water effects into account. Instead, approaches which are resolving the flow around the vessel may be used to quantify the vessel performance in restricted waters.

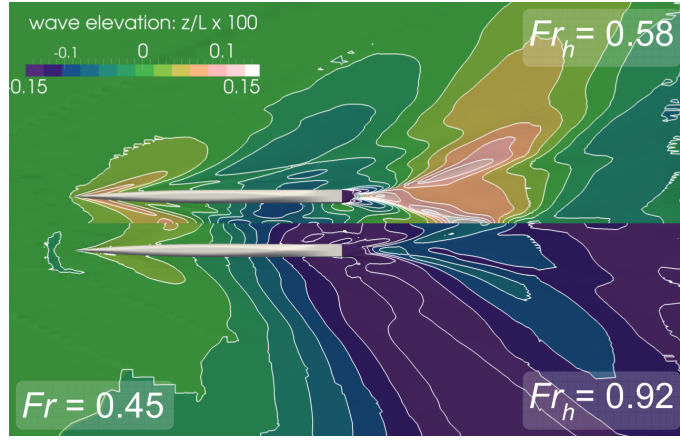


Figure 13: Wave contour of the 130 m catamaran at 1:50 model scale  $Fr = 0.45$ . Top:  $h/L = 0.6$ ,  $Fr_h = 0.58$ . Bottom:  $h/L = 0.24$ ,  $Fr_h = 0.92$ .

#### 4.4 Practical Implications

In Section 2.2 it was shown that the drag force in towing tank with restricted water can be predicted within 6% for the heavy displacement case and even within 3% for light displacement case when compared to measurements. Furthermore the CFD approach has been capable of quantifying the influence of limited depth and width on the total drag force compared to an infinitely deep and wide tank (Section 3.1). Especially for medium-speed catamarans with high slenderness ratios the effect of blockage is considered as being small as the midship sectional area is small with respect to the towing tank cross section when compared to conventional craft of comparable displacement. Hence the CFD approach can be used to design towing tank experiments so that the influence of the tank bottom or walls is below a specified threshold when a maximum model scale factor is applied. Also the unsteady effects such as the increase in oscillation period of the model response can be considered in the simulations, which allows to estimate if a sufficient number of oscillation cycles will be recorded and thus a converging solution can be achieved. This emphasises the applicability of CFD as a model-ship correlation tool as proposed in an earlier study [12].

## 5 Conclusions

This study used numerical simulations, model test data and full-scale measurements to investigate steady and unsteady finite water effects. The numerical model was verified using towing test experiments, and CFD underestimated drag at the light displacement condition by as little as 3% for Froude numbers of  $Fr = 0.37$  and 0.45 and under estimated the drag by less than 6% at the combination of heavy displacement and higher speed.

Firstly, steady finite water no matter if restricted in depth or width was found to increase the calm water resistance force, an effect that can be attributed to blockage and increased wave making, especially in limited water depth. For a fixed domain or towing tank width of  $b/L = 1.4$  a depth of  $h/L = 0.7$  and 0.8 is required at Froude numbers of  $Fr = 0.37$  and 0.45 for the residuary resistance being less than 1% above the value for an infinitely deep fluid domain. For shallow water depths such as  $h/L = 0.24$  the domain width was found to be at least  $b/L = 1.2$  for speeds of  $Fr = 0.37$  to not exceed the residuary resistance for an infinitely wide domain by more than 1%, For Froude numbers of  $Fr = 0.45$  the required widths increases to  $b/L = 15.6$ .

Secondly, unsteady finite water effects mainly related to a reduced water depth and were found to be of very high importance for large medium-speed vessels. These effects lead to an increase in the oscillations in resistance and measured heave and trim that occur at periods in excess of the available runtime in towing tank experiments. Therefore, the averaging of the transient data record may lead to inaccurate results. The dimensionless period of these oscillations has been shown to have agreement between numerical predictions, towing tank experiments and full-scale sea trial measurements. The non-dimensional frequency solely depends on vessel length and depth Froude number.

When comparing full-scale drag for a medium-speed catamaran in limited water depth ( $h/L = 0.12-0.17$ ) predictions by CFD to results from sea trials and extrapolated deep water model test data, it was found that CFD estimates are 15% larger than extrapolated model test data, but up to 32% smaller when compared to powering data from sea trials. It has been concluded that shallow water corrections for model test data does not deliver reliable results and that the propulsor size needs to be larger than the resistance value would suggest.

Full-scale resistance prediction using a novel CFD-approach for 130 m catamaran at Froude number of  $Fr = 0.37$  delivered a 13% higher drag when compared to extrapolated model test data recorded at the corresponding water depth, but at the Froude number of  $Fr = 0.45$  the CFD prediction was 4% lower. Pressure related forces from CFD predictions for a sufficiently wide fluid domain were up to 12% lower and

frictional forces up to 35% higher when compared to extrapolated model-scale data.

This emphasises the requirement for reliable full-scale drag prediction to estimate the power requirements, especially if the ship is operated in shallow water. It has been shown that deep water towing tank tests results corrected for shallow water effects using ITTC recommended procedures underestimated the drag force when compared to CFD predictions. Also, extrapolating shallow water data using approaches mentioned for deep water may lead to an underestimate of the total drag force at full scale.

Finally, it has been suggested that the CFD approach can be utilised to evaluate model sizes for towing tank testing to keep the influence of steady and unsteady finite water effects on the drag force to an agreed minimum.

## 5.1 Recommendations for Future Work

Future work may focus on further validation approaches. These could include modelling the waterjet unit to enhance the methodological correlation when comparing results to full-scale sea trial data or to exactly replicate the acceleration of the towing tank carriage and limited tank length to avoid using time averaged values for validation at model-scale which may lead to inaccurate results as the average may have been determined from too few oscillation cycle of the ship model response.

## 6 Acknowledgements

I would like to thank Jack Bucher, Prof Michael R. Davis, Prof Lawrence Doctors, Dr Shinsuke Matsubara and Dr Jalal Rafie Shahraki for their inspiration, support and discussions on unsteady finite water effects as well as Michiel Verhulst from *MARIN*, Stuart Friezer from *Stuart Friezer Marine*, and Tim Lilienthal from the *AMC* towing tank for providing data records to support this study.

This research has been conducted as part of a collaborative research project between INCAT, Revolution Design, MARIN, Wärtsilä, and the School of Engineering and the Australian Maritime College at the University of Tasmania. It was supported under Australian Research Council's Linkage Projects funding scheme (project number LP110100080).

## References

- [1] Davidson G, Roberts TR, Friezer S, Davis MR, Bose N, Thomas G, et al. Maximising Efficiency and Minimising Cost in High Speed Craft. In: International Conference on Fast Sea Transportation. vol. 11; 2011. p. 727–734.
- [2] Haase M, Davidson G, Friezer S, Binns J, Thomas G, Bose N. On the Macro Hydrodynamic Design of Highly Efficient Medium-speed Catamarans with Minimum Resistance. Transaction of the Royal Institution of Naval Architects, Part A - International Journal of Maritime Engineering. 2012;154(A3):131–142.
- [3] Haase M, Davidson G, Friezer S, Binns J, Thomas G, Bose N. Hydrodynamic Hull Form Design Space Exploration of Large Medium-Speed Catamarans Using Full-Scale CFD. Transaction of the Royal Institution of Naval Architects, Part A - International Journal of Maritime Engineering. 2015;in press.
- [4] Schuster S. Beitrag zur Frage der Kanalkorrektur bei Modellversuchen (in German). Schiffstechnik. 1956;p. 93–96.
- [5] Tamura K. Study of the Blockage Correction. Journal of the Society of Naval Architects of Japan. 1972;131:17–28.
- [6] Wehausen JV. Effect of the initial acceleration upon the wave resistance of ship models. Journal of Ship Research. 1964;7(3):38–50.
- [7] Day AH, Clelland D, Doctors LJ. Unsteady finite-depth effects during resistance tests on a ship model in a towing tank. Journal of Marine Science and Technology. 2009;14(3):387–397.
- [8] Davidson G, Roberts TR, Friezer S, Thomas G, Bose N, Davis MR, et al. 130m Wave Piercer Catamaran: A New Energy Efficient Multihull Operating at Critical Speeds. In: Proceedings of International RINA Conference on High Speed Marine Vehicles; 2011. p. 61–72.
- [9] Griggs D, Woo E. HSV-2 SWIFT Combined Standardization and Powering Trials Results . Naval Surface Warfare Center, Carderock Division; 2005.
- [10] Tezdogan T, Incecik A, Turan O. A Numerical Investigation of the Squat and Resistance of Ships Advancing through a Canal using CFD. Journal of Marine Science and Technology. 2015;20:1–16.
- [11] Castiglione T, He W, Stern F, Bova S. URANS simulations of catamaran interference in shallow water. Journal of Marine Science and Technology. 2013;19:33–51.



- [12] Haase M, Zürcher K, Davidson G, Binns J, Thomas G, Bose N. Novel CFD-Based Full-Scale Resistance Prediction for Large Medium-Speed Catamarans. *Ocean Engineering*. 2016;111:198–208.
- [13] Zürcher K. Waterjet Testing Techniques for Powering Performance Estimation using a Single Catamaran Demihull. University of Tasmania; 2016.
- [14] Havelock TH. The Wave Resistance of a Cylinder Started from Rest. Oxford University Press. 1949;.
- [15] Matsubara S. Ship Motions and Wave-Induced Loads on High Speed Catamarans. University of Tasmania; 2011.
- [16] Bucher J. Calm Water Pitch Motions of Large Medium-speed Catamarans [BEng Thesis]. University of Tasmania; 2014.
- [17] Oura T, Ikeda Y. Maneuverability of a Wavepiercing High-Speed Catamaran at Low Speed in Strong Wind. In: *Proceedings of International Conference on Marine Research and Transportation*; 2008. p. 17–20.